Spatial and Spatio-temporal Epidemiology 49 (2024) 100650

Contents lists available at ScienceDirect

Spatial and Spatio-temporal Epidemiology

journal homepage: www.elsevier.com/locate/sste

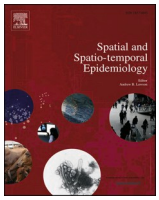

# Predicting the odds of chronic wasting disease with Habitat Risk software

W. David Walter [a,*], Brenda Hanley [b], Cara E. Them [c], Corey I. Mitchell [d,†], James Kelly [e,‡], Daniel Grove [e], Nicholas Hollingshead [b], Rachel C. Abbott [b], Krysten L. Schuler [b]

[a] U.S. Geological Survey, Pennsylvania Cooperative Fish & Wildlife Research Unit, The Pennsylvania State University, University Park, Pennsylvania, 16802, USA
[b] Wildlife Health Lab, Cornell University, 240 Farrier Road, Ithaca, NY, 14853, USA
[c] Cara Them Consulting, LLC, Corvallis, 973300, USA
[d] Desert Centered Ecology, LLC, Tucson, AZ, 85716, USA
[e] Tennessee Wildlife Resources Agency, Nashville, Tennessee, 37211, USA

ARTICLE INFO

*Keywords:*
Chronic wasting disease
CWD
Habitat
*Habitat Risk*
Epidemiology
*Odocoileus virginianus*
Environmental modeling
Semi-automated software
White-tailed deer
Wildlife health

ABSTRACT

Chronic wasting disease (CWD) is a transmissible spongiform encephalopathy that was first detected in captive cervids in Colorado, United States (US) in 1967, but has since spread into free-ranging white-tailed deer (*Odocoileus virginianus*) across the US and Canada as well as to Scandinavia and South Korea. In some areas, the disease is considered endemic in wild deer populations, and governmental wildlife agencies have employed epidemiological models to understand long-term environmental risk. However, continued rapid spread of CWD into new regions of the continent has underscored the need for extension of these models into broader tools applicable for wide use by wildlife agencies. Additionally, efforts to semi-automate models will facilitate access of technical scientific methods to broader users. We introduce software (*Habitat Risk*) designed to link a previously published epidemiological model with spatially referenced environmental and disease testing data to enable agency personnel to make up-to-date, localized, data-driven predictions regarding the odds of CWD detection in surrounding areas after an outbreak is discovered. *Habitat Risk* requires pre-processing publicly available environmental datasets and standardization of disease testing (surveillance) data, after which an autonomous computational workflow terminates in a user interface that displays an interactive map of disease risk. We demonstrated the use of the *Habitat Risk* software with surveillance data of white-tailed deer from Tennessee, USA.

## 1. Introduction

Chronic wasting disease (CWD) is a transmissible spongiform encephalopathy that is lethal to cervids and was first detected in mule deer (*Odocoileus hemionus*) in Colorado, United States (US) in 1967 (Williams and Young, 1980). In addition to mule deer, CWD affects numerous cervid species that include: white-tailed deer (*Odocoileus virginianus*), elk (*Cervus canadensis*), and moose (*Alces alces*), all of which constitute important sources of high quality, locally sourced meat to US residents ([USGS], 2023). Chronic wasting disease has since been discovered in additional areas across North America and at present is confirmed to exist in free-ranging cervid populations in 31 US states, three Canadian provinces, and three Scandinavian countries ([USGS], 2023). Knowledge of the status, distribution, and spread of CWD in free-ranging cervid populations is important to wildlife agencies tasked with permitting cervid harvest and managing towards sustainable cervid populations in the presence of the disease. While US state wildlife agencies are not public health agencies (and the consumption of infectious prions from wild game is not currently known to be deleterious to human health ([CDC], 2021), human health agencies in North America have recommended that no part of a CWD positive cervid be consumed by humans, rendering dissemination of risk of disease to humans a

* Corresponding author.
*E-mail address:* wdw12@psu.edu (W.D. Walter).
† Current address: Desert Tortoise Recovery Office, U.S. Fish and Wildlife Service, Tucson, Arizona, 85745, USA.
‡ Current address: Florida Fish and Wildlife Conservation Commission 1105 SW Williston Rd Gainesville, FL 32601.

https://doi.org/10.1016/j.sste.2024.100650
Received 21 August 2023; Received in revised form 4 March 2024; Accepted 9 April 2024
Available online 11 April 2024

highly important topic of communication between agencies and the public ([CDC], 2021).

Since discovery of CWD in wild cervids in the 1980s, US state and Canadian provincial wildlife agencies have regularly conducted disease surveillance of free-ranging cervid populations to detect infections and evaluate disease trajectories ([USGS], 2023). Over the years, traditional epidemiological models have been used with disease surveillance data and enhanced by the incorporation of habitat covariates (Mollison, 1977; Hethcote, 1989). Tissue samples frequently used as data inputs to these models are largely sourced from hunter-harvested animals, which results in several statistical disadvantages that renders traditional analyses challenging. Statisticians have overcome some of these challenges by adopting a Bayesian hierarchical approach to epidemiological models (Gelman et al., 2004). At present, such analytical infrastructure was commonly used to investigate wildlife disease in cervids throughout the US (Farnsworth et al., 2006; Osnas et al., 2009; Walter et al., 2011, 2014) and continues to aid study and management of wildlife disease in free-ranging populations. Despite their applicability and utility, these methods require a specific and detailed framework for appropriate application to real world data, creating a barrier for use by wildlife managers.

As CWD spreads into new areas and opportunistic sampling remains the primary sampling methodology, the benefits of the application of Bayesian hierarchical models to understand and communicate disease risk in free-ranging wildlife have become evident, but Bayesian modeling can be a challenging proposition for agencies. Models are often time consuming and computationally expensive to create and run, and not all agencies have personnel with appropriate quantitative training. Many agencies collect the same type of data, often using similar (or identical) methodologies ([AFWA], 2018; [CWHL], 2021), which increases potential for interagency cooperation regarding data collection, analysis and ultimately coordination of management to mitigate shared threats of the disease. Therefore, the current potential for widespread analysis using a Bayesian tool appears to be limited, not by the availability of data and their comparability, nor by the willingness for cooperation, but by the difficulties and costs associated with performing the analyses. We addressed this gap by developing, *Habitat Risk*, software to provide a workflow to reduce the technical acumen required to conduct the predictable steps of a Bayesian hierarchical modeling process. This workflow provides interested agencies with the capacity to overcome current barriers to use and benefit from these powerful models using their own disease surveillance data.

In this paper we present *Habitat Risk,* a step-by-step workflow of previously published Bayesian hierarchical analysis to compute the odds that a white-tailed deer (hereafter referred to as *deer*) harvested in a given location will test positive for CWD based on covariates that reflect CWD risk (Farnsworth et al., 2006; Osnas et al., 2009; Walter et al., 2011, 2014). *Habitat Risk* was created as a collaboration with state agencies and Cornell Wildlife Health Laboratory ([CWHL], 2021) with each participating state and a detailed tutorial made available (Hanley et al., 2021). The paper is organized as steps in a workflow as follows. In Section 2, we connect disease surveillance to environmental data within a sampling grid to provide a sampling dataset in program R (R Core Team, 2020). In Section 3, we prepare the sampling dataset then estimate parameter values of 25 possible (pre-specified) candidate models using *WinBUGS* (Lunn et al., 2000) followed by model selection and summary results of the best model. Finally, in Section 4, we return results via an interactive user interface to display risk of infection across the study area. While the predictable steps of the Bayesian hierarchical analysis are contained in the software, duties of a user of our workflow without our example dataset and layers provided include collection of disease surveillance data, initial gathering of publicly available environmental data, and verification that the model ran as intended through confirmation that Markov chains converged through appropriate interpretation of the modeling diagnostics. Finally, we conclude with options and steps for future improvements or additional analyses that could utilize similar workflows.

## 2. Habitat risk workflow

*Habitat Risk* requires the user to input location-specific data in the form of *disease surveillance* and *environmental* data using script: *1_Tennessee_Data_Prep. Disease surveillance* data contain CWD sampling records that include results on the CWD status of each deceased individual deer (positive test or not detected). D*isease surveillance* data are generated by hunters, the agency, and its partners from these deer, with CWD status verified by an accredited diagnostic laboratory using an enzyme-linked immunosorbent assay on the obex or retropharyngeal lymph nodes with secondary confirmation testing of positive detection using immunohistochemistry (Williams et al., 2002; Keane et al., 2008). *Disease surveillance* data further includes demographic information on each deer, such as age, sex, and location of harvest. *Disease surveillance* variables were selected *a priori* for inclusion in the dataset because of previous findings of associations between CWD and male deer and increased prevalence of CWD in older individuals (Miller and Conner, 2005; Grear et al., 2006). Sex is defined as male or female and is verified by the agency. Age is estimated by trained agency biologists using the tooth replacement and wear method (Severinghaus, 1949) or through the interpretation of annuli in the cementum of the first incisor (Gilbert, 1966). Location is defined as the spatial coordinates, *latitude* and *longitude*, of harvest and was selected because the proximity to a previously detected CWD infection is known to influence disease risk in new detections (Farnsworth et al., 2006; Osnas et al., 2009; Walter et al., 2011, 2014). Location references the harvest location of the deer, as provided by the hunter to the agency. *Habitat Risk* assumes that the transfer and testing of tissues from hunter-harvested deer, including designations of *sex* and *age* for each deer, as well as the accuracy and precision of the location data, were overseen by the agency, and assumes that the resulting records are both accurate and statistically comparable. A detailed tutorial including directions to gather and pre-process *environmental* data are available (Mitchell et al., 2021), while a detailed tutorial including directions to prepare *disease surveillance* data for linkage with *environmental* data for processing within *Habitat Risk* also are available (Hanley et al., 2021).

### 2.1. Data preparation - disease surveillance data

Chronic wasting disease was first detected in wild deer in eastern Tennessee, USA in 2018, following implementation of a risk-based weighted surveillance plan by the Tennessee Wildlife Resource Agency (TWRA; Schuler et al., 2018). Surveillance data collected in the area since 2018 includes all deer samples submitted to TWRA by the hunting public. Data were cleaned by TWRA in a process internal to the agency prior to being made available for use in *Habitat Risk*. Total *disease surveillance* data for deer provided by the TWRA for this study spanned the 2018–2019 hunting season through the 2020–2021 hunting season and included 14,856 deer tested for CWD: 44.2 % tested were female; 55.7 % tested were male; 0.01 % tested had sex unknown; 62.6 % tested were adults (>23 months of age); 24.0 % tested were yearlings (12–23 months of age); 9.8 % tested were fawns (<12 months of age); 3.6 % tested had no age ([TWRA], 2023). Of the 14,856 tested deer, 5.0 % were CWD positive: 27.2 % were positive females; 72.5 % were positive males; 0.3

% positives had sex unknown; 81.3 % positives were adults; 11.8 % positives were yearlings; 1.9 % positives were fawns; 5.0 % positives had no age ([TWRA], 2023). Harvest locations were provided in *latitude* and *longitude* by hunters providing the samples and assumed by TWRA to be exact.

As an example dataset, we have provided locations for the *disease surveillance* data for Tennessee, USA within their Unit CWD that was established in 2018 ([TWRA], 2023). Due to data privacy concerns, we do not provide the true locations of samples collected, rather provide this data as randomly offset 100 m in both latitude and longitude. To date, county-level prevalence for CWD in western Tennessee ranges from <1 % to 18.6 % with the highest county prevalence occurring in Fayette County where CWD was initially discovered in 2018.

### 2.2. Data preparation – sampling grid

The Bayesian hierarchical model was fitted to *disease surveillance* and *environmental* data via a spatial sampling grid as previously described (Farnsworth et al., 2006; Walter et al., 2011; Evans et al., 2016). Because many states and provinces in eastern North America do not have data to estimate the home range of resident deer, our workflow used a grid cell resolution based on size of an average home range of 6 $km^2$ that was based on previous research on deer in the eastern US (Evans et al., 2016; Walter et al., 2018), although our code allows for the flexibility to alter this grid size to the study area of interest. To minimize distortion, the sampling grid was initiated in the State Plane Coordinate System of 1983 zone specific to the area of interest (Stem, 1990), which was defined based on processed *environmental* data (Mitchell, 2021). The sampling grid was created and maintained for use in additional steps in the workflow outlined below.

The sampling grid selected for this case study was centered on the CWD outbreak in deer in southwestern Tennessee, covering part of Hardeman and Fayette counties (Fig. 1). The area covered by the sampling grid was determined by the nature of the outbreak; we included all positive CWD samples in the outbreak zone and a small buffer. The sampling grid contained 837 grid cells, representing a total area of 5022 $km^2$ (6 $km^2$ per cell × 837 cells). Not all deer in the total *disease surveillance* data were harvested in locations within the sampling grid, so we omitted those deer with harvest locations outside of the sampling grid. Thus, our analysis included harvest locations for 5284 deer: 9.9 % of deer in the grid were CWD positive; 43.3 % of deer in the grid were female; 56.7 % of deer in the grid were male; 66.1 % of deer in the grid were adults; 23.8 % of deer in the grid were yearlings; 10.0 % of deer in the grid were fawns. Deer that fell within the grid but their sex or age was unknown were omitted. Because this subset of data is for less than half of the surveillance dataset available and only collected over a short duration of years, this dataset was made available for demonstration of our software only and results were not considered suitable for and were not intended to direct CWD management in Tennessee.

### 2.3. Data preparation - environmental data

*Environmental* data matches landscape characteristics to *disease surveillance* data. *Environmental* data includes elevation, slope, land cover, streams, and clay that were selected *a priori* for inclusion in the dataset because selection for these attributes is important for understanding drivers of CWD (Farnsworth et al., 2006; Walter et al., 2011; Storm et al., 2013; Evans et al., 2016). We obtained *environmental* data from multiple publicly available datasets and created layers used for inputs with program R (R Core Team, 2020) using *Geoprocessing* software (Mitchell, 2021).

Land cover classes were combined to cover three land cover categories (forest, open, developed) and derived from National Land Cover Database 2016 (NLCD; Dewitz, 2019). Forest included deciduous, evergreen, and mixed forest cover areas as well as shrubland and wetlands (NLCD classes 41, 42, 43, 51, 52, 90, and 95). Open represented

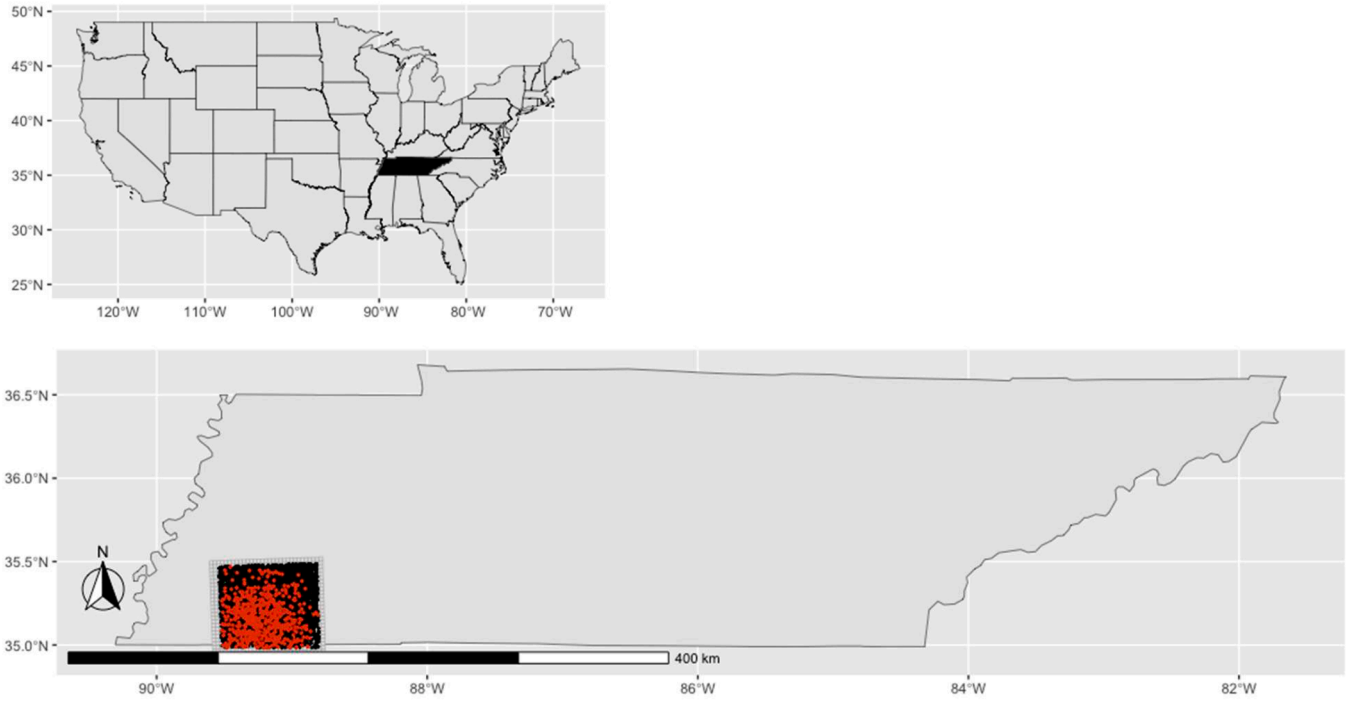


**Fig. 1.** The study area used by the *Habitat Risk* software to infer the presence of chronic wasting disease (CWD) in white-tailed deer in Tennessee, USA (Outset). The hatched grid represented the study area, the red points within the hatched grid indicated locations of CWD positive samples, while black points within the hatched grid indicated locations of samples not detected for CWD (Inset). Additional *disease surveillance* samples with a harvest location that did not fall within the sampling grid have been omitted from this figure.

pasture, cultivated crops, and grasses (NLCD classes 71–74, 81, 82). Developed included urban, suburban, and barren areas (21–24, 31). Land cover categories were presented as proportions of each category within each cell of the sampling grid based on an area-weighted mean. Because forest, open, and developed were highly correlated (Pearson's $|r| > 0.7$; Zar, 1996), we selected forest to represent land cover due to the strong relationship of forest with distribution of CWD (Evans et al., 2016). Land cover categories were selected because previous research identified agricultural-forest matrices influenced deer densities, which likely contributed to spread of CWD at the local scale (Storm et al., 2013; Kelly et al., 2014).

Elevation (hereafter dem) was defined as average elevation (m) above sea level, as attained from the 30-meter National Elevation Dataset (Gesch, 2007). Slope was defined as the change in elevational gradient (degrees) and was derived from dem which was computed using previous methods (Horn, 1981). Streams were selected because large rivers were considered barriers to movement of disease or gene flow in various regions (Hefley et al., 2017; Miller et al., 2020). Streams were presented as distance (m) to medium-large streams and rivers from the National Hydrography Dataset Plus Version 2 (McKay, 2012). Medium-large streams were identified as Strahler order of four or higher based on previous gene flow assessment in the eastern US (Miller et al., 2020). Clay was selected because this substrate was known to be a significant predictor of CWD in various states (Walter et al., 2011), although not necessarily in the eastern US (Evans et al., 2016). Clay represented the percent clay in the upper 50 cm of the soil as derived from the Gridded National Soil Survey Geographic Database (Soil Survey Staff, 2020) using an approach previously described (Wieczorek, 2014). The *environmental* data were pre-processed for the extent of the state of Tennessee using *Geoprocessing* software (Mitchell, 2021) then cropped to reflect the spatial extent of the sampling grid described above.

### 2.4. Data preparation - assignment and extraction

Environmental data layers were combined into a raster stack which are then summarized within each cell of the sampling grid. The area-weighted average of each *environmental* variable was calculated for each 6 $km^2$ sampling grid cell and values were assigned to each deer based on recorded location within a cell following the assumption that the recorded harvest location was representative of its natural home range (Evans et al., 2016). A final dataset was prepared that combines disease surveillance and environmental data for each deer sampled as well as sampling grid identification necessary for Bayesian hierarchical modeling.

## 3. Bayesian hierarchical models

### 3.1. Model parameters

*Habitat Risk* requires the user to implement models within *WinBUGS* (Lunn et al., 2000) using R2WinBUGS (Sturtz et al. 2005) automated in the script: *2_Tennessee_PipelineParallel*. We assumed that CWD was distributed in an environmentally heterogenous mosaic across the landscape (Farnsworth et al., 2006; Osnas et al., 2009; Walter et al., 2011), so our workflow combined *disease surveillance* and *environmental* data as described above in a framework appropriate for Bayesian hierarchical modeling. Our workflow is meant to facilitate well established principles, practices, and assumptions of Bayesian hierarchical models (Banerjee et al., 2004; Gelman et al., 2004), thus we do not intend to present equations or background for these fundamental principles that are provided in citations therein. Briefly, the principles of our workflow follow those of Bayes' theorem (i.e., Bayesian analyses) that combines prior probability distributions with likelihood to determine posterior distribution of parameters (Banerjee et al. 2004). Implementation of spatial and spatial-temporal models is often prohibitive with use of standard methods but is possible with MCMC that allows us to estimate posterior distributions. Furthermore, Bayesian hierarchical modeling with logistic regression and adjusted covariates (Spiegelhalter et al., 2002) has been described multiple times to compute the odds that a harvested deer in any given location will be disease positive (Farnsworth et al., 2006; Walter et al., 2011; Evans et al., 2016) by estimating the similarities of a cell of interest with the bulk of cells found positive.

**Table 1**
Set of 25 candidate models determined *a priori* and used by *Habitat Risk* to investigate the effect of demographic and environmental covariates on odds of chronic wasting disease infection. The *Intercept* corresponds to the baseline class (fawn female); *sex* is coded as male = 1 and female = 0; *age* is coded as fawn = 0, yearling = 1, and adult = 2. Environmental covariates include *dem*, the digital elevation model; *slope*, the localized gradient of the area; *for*, a compound category representing forest cover (which is highly correlated with the percentage of open and developed land covers such that *open* and *developed* covariates have been omitted from the analysis); *streams*, the distance (meters) to the nearest water source; and *clay*, the percentage of clay in the soil. Environmental effects further include local clustering of the disease (*CAR*) and region-wide heterogeneity of the disease (*HET*).

| Model | Model Structure |
|---|---|
| 1 | Intercept + sex + age + dem + slope + for + streams + clay + CAR + HET |
| 2 | Intercept + sex + age + dem + slope + — + streams + clay + CAR + HET |
| 3 | Intercept + sex + age + dem + —— + for + streams + clay + CAR + HET |
| 4 | Intercept + sex + age + —— + slope + for + streams + clay + CAR + HET |
| 5 | Intercept + sex + age + dem + —— + — + streams + clay + CAR + HET |
| 6 | Intercept + sex + age + —— + slope + — + streams + clay + CAR + HET |
| 7 | Intercept + sex + age + —— + —— + for + streams + clay + CAR + HET |
| 8 | Intercept + sex + age + —— + —— + — + streams + clay + CAR + HET |
| 9 | Intercept + sex + age + —— + —— + — + ——— + clay + CAR + HET |
| 10 | Intercept + sex + age + —— + —— + — + streams + — + CAR + HET |
| 11 | Intercept + sex + age + —— + —— + — + streams + clay + —— + HET |
| 12 | Intercept + sex + age + —— + —— + — + streams + clay + CAR + — |
| 13 | Intercept + sex + age + —— + —— + — + —— + —— + CAR + HET |
| 14 | Intercept + sex + age + —— + —— + — + ——— + clay + —— + HET |
| 15 | Intercept + sex + age + —— + —— + — + ——— + clay + CAR + — |
| 16 | Intercept + sex + age + —— + —— + — + streams + — + —— + HET |
| 17 | Intercept + sex + age + —— + —— + — + streams + —— + CAR + — |
| 18 | Intercept + sex + age + —— + —— + — + streams + clay + —— + — |
| 19 | Intercept + sex + age + —— + —— + — + ——— + —— + — + HET |
| 20 | Intercept + sex + age + —— + —— + — + ——— + —— + CAR + — |
| 21 | Intercept + sex + age + —— + —— + — + ——— + clay + —— + — |
| 22 | Intercept + sex + age + —— + —— + — + streams + —— + —— + — |
| 23 | Intercept + sex + age + —— + —— + — + ——— + —— + —— + — |
| 24 | Intercept + — + — + —— + —— + — + —— + —— + CAR + HET |
| 25 | Intercept + — + — + —— + —— + — + —— + —— + —— + — |

### 3.2. Spatial random effects

We further defined random effects to capture the influence of clustering in the local neighborhood (i.e., grid cells sharing borders or vertices; hereafter *CAR*) and the heterogeneous influences occurring at the resolution of the grid cell (hereafter *HET*; Banerjee et al., 2004). We initiated different combinations of parameters (*disease surveillance, environmental, CAR,* and *HET*) within the Bayesian hierarchical framework to construct, *a priori*, 25 candidate model structures of additive *surveillance* and *environmental* effects. We compared the suitability of the 25 candidate models given the data (Table 1), then used model selection techniques to determine the best model for that data (i.e., that

mathematical structure that generates the lowest relative deviance information criterion (DIC) given the data; (Burnham and Anderson, 2002; Spiegelhalter et al. 2002; Farnsworth et al. 2006). To estimate infection odds by sample segment, all structures contained *age* and *sex* as necessary covariates. The exact list of candidate structures was further developed using unique combinations of remaining *environmental* variables with and without the inclusion of the spatial effects *CAR* and *HET* (Table 1). Within the sampling grid, estimates for parameter values given the data for the 25 candidate models were calculated using the following equation:

$$\text{logit}(\varphi_{ij}) = \mu + \beta_1 sex + \beta_2 age + CAR_j. \quad (1)$$

The posterior estimates of the parameters ($\mu$, $\beta_1$, $\beta_2$) of eq. (1) are displayed in The Best Model. Each model ran for $\leq$ 36 *h*, for a total runtime of ~14 days when run in sequence (or ~2 days if all 25 models were run in parallel).

### 3.3. Model priors and diagnostics

Priors for Markov chain Monte Carlo (MCMC) reflected those used in Eberly and Carlin (2000), Walter et al. (2014), and Evans et al. (2016), which included the non-informative prior distributions $N$ (0, 100,000) for each $\beta$ and an improper (flat) prior over the entire real line $U(-\infty, \infty)$ for $\mu$. Models were fitted with data using five independent Markov chains that had been initialized at random, run for 150,000 iterations (with the first 50,000 discarded as burn-in), then thinned to every 20th iteration. These parameterization settings were selected because higher numbers of iterations were unable to run due to storage constraints, so our settings were troubleshooted through examination of similar models in the literature (Ferreira et al. 2016).

We generated diagnostic plots for the best model. Diagnostic plots included convergence diagnostics (Geweke, 1992; Gelman et al., 2004; Heidelberger and Welch, 1983; Raftery and Lewis, 1992), trace plots (Sturtz et al., 2005; Roy, 2020), and correlation plots (Plummer et al., 2006; Sturtz et al., 2005). We verified that the MCMC methods had performed as expected for the best model. While *HET* and *CAR* were programmed into models in *Habitat Risk*, omitted from the computations were parameters such as *psi*, the ratio of the standard deviation of *CAR* to combined standard deviations of *CAR* and *HET*, which has been used to assess how each environmental effect accounted for variability that was not accounted for by environmental effects (Eberly and Carlin, 2000; Evans et al., 2016). Such detailed analyses of this variability exceed the capabilities of *Habitat Risk* but may be an important consideration. As well, emerging scientific information may alter the potential covariate candidates, rendering the use of environmental covariates *dem, slope, forest, streams*, and *clay* too narrow. For example, derivatives of *forest*, such as the distinction between deciduous, evergreen, or mixed forest types may be hypothesized to have further predictive power for CWD infection. A programmer may replace raster layers in *Habitat Risk*, but these modifications are not accommodated currently. Any time a new raster layer or dataset other than those accommodated in the software is used, prior distributions of the new coefficients should be carefully considered. Similarly, the user may wish to modify home range size, which is also achievable by modifying the original code. In summary, it is important that *Habitat Risk* be seen as a flexible tool that can be used as is, updated to reflect new environmental information, or modified to investigate hypotheses in specific jurisdictional areas.

**Table 2**
Model comparisons in the *Model Selection* tab of the *Habitat Risk* software given data from Tennessee, US. *Deviance* represents the posterior mean of the deviance (Evans et al. 2016); p*D* represents the effective number of parameters in the posterior distribution (equal to the variance of the deviance divided by 2; Sturtz et al. 2005); DIC represents the Deviance Information Criterion (Spiegelhalter et al. 2002); *Change in DIC* represents the difference between the DIC value and the smallest DIC value among all models compared (Evans et al. 2016). The best model for the Tennessee, US was Model 20. A table with the same structure will auto-populate on the *Model Selection* tab of the *Habitat Risk* software when data from other locations are used.

| Model | Deviance | pD | DIC | Change in DIC |
|---|---|---|---|---|
| Model 20 | −1.31 | 1.04 | 3060.79 | 0 |
| Model 17 | −1.33 | 1.05 | 3060.98 | 0.19 |
| Model 15 | −1.39 | 1 | 3061.54 | 0.75 |
| Model 12 | −1.41 | 1 | 3061.76 | 0.97 |
| Model 10 | −1.35 | 0.96 | 3065.42 | 4.63 |
| Model 13 | −1.31 | 0.97 | 3065.94 | 5.15 |
| Model 9 | −1.4 | 0.96 | 3066.12 | 5.32 |
| Model 6 | −1.34 | 0.95 | 3066.47 | 5.68 |
| Model 8 | −1.42 | 0.96 | 3066.72 | 5.93 |
| Model 7 | −1.33 | 0.96 | 3067.49 | 6.7 |
| Model 4 | −1.28 | 0.98 | 3067.86 | 7.07 |
| Model 5 | −0.91 | 0.85 | 3068.16 | 7.37 |
| Model 3 | −0.86 | 0.86 | 3069.23 | 8.44 |
| Model 2 | −0.91 | 0.86 | 3069.8 | 9.01 |
| Model 1 | −0.75 | 0.86 | 3071.28 | 10.49 |
| Model 24 | −1.32 | 0.92 | 3254.43 | 193.64 |
| Model 11 | −0.01 | 0.81 | 3274.81 | 214.02 |
| Model 16 | 0 | 0.85 | 3279.92 | 219.13 |
| Model 14 | 0.01 | 0.84 | 3283.38 | 222.59 |
| Model 19 | 0.01 | 0.83 | 3287.62 | 226.82 |
| Model 18 | 3776.66 | 5.24 | 3781.73 | 720.94 |
| Model 21 | 3791.97 | 4.15 | 3795.98 | 735.19 |
| Model 22 | 3799.36 | 3.96 | 3803.36 | 742.56 |
| Model 23 | 3813.64 | 3.09 | 3816.65 | 755.86 |
| Model 25 | 4000.31 | 1.1 | 4001.3 | 940.51 |

Model 20 (containing explanatory variables *age, sex*, and *CAR*) had the lowest relative DIC when compared to the other candidate models (DIC = 3060.79; Table 2).

Models 17, 15, and 12 have a DIC similar to Model 20. Unlike Models 17, 15, and 12, which contained demographic (*sex* and *age*) and spatial effect *CAR*, plus the environmental covariates *clay* (Model 15), *streams* (Model 17), or both *clay* and *streams* (Model 12), Model 20 contained only the spatial effects of the demographics and *CAR*. We note that the estimates of $CAR_j$ are not displayed because the estimates are cell specific, however, these estimates are saved internally by the software to ensure that grid-specific odds are accurately computed. Diagnostics revealed that the Markov chains became independent of initial conditions and all parameters converged to their stationary posterior distributions. We do not include the diagnostic plots here, but they are generated and displayed to the user each time *Habitat Risk* is used. *Relative risk* revealed that adult males carry the highest risk of CWD infection in southwestern Tennessee when compared to other population segments of deer, and the southcentral area within the sampling grid yielded the highest odds of infection compared to the other grid cells adjacent to or distal to the outbreak.

## 4. Habitat risk r shiny app

The terminus of *Habitat Risk* is a Shiny web application (Chang, 2016) that displays results of the modeling process using the script: *3_Tennessee_HabitatRisk*. Seven menu tabs include (1) *Maps of All Deer Tested*, (2) *Maps of deer that test positive for CWD (CWD+ Deer)*, (3) *Relative Risk Maps*, (4) *Model Selection*, (5) *The Best Model*, (6) *Export the Relative Risk Maps*, and (7) *Tutorial*.

### 4.1. Maps of all deer tested

*Maps of All Deer Tested* tab overlays *disease surveillance* data over the raster images of *elevation, slope, forest, streams, clay, open*, and *developed* in the study area. *Disease surveillance* data may be further partitioned by selecting by CWD test *result, sex,* or *age*.

### 4.2. Maps deer positive for cwd

*Maps of CWD+ Deer* tab overlays the *disease surveillance* data for

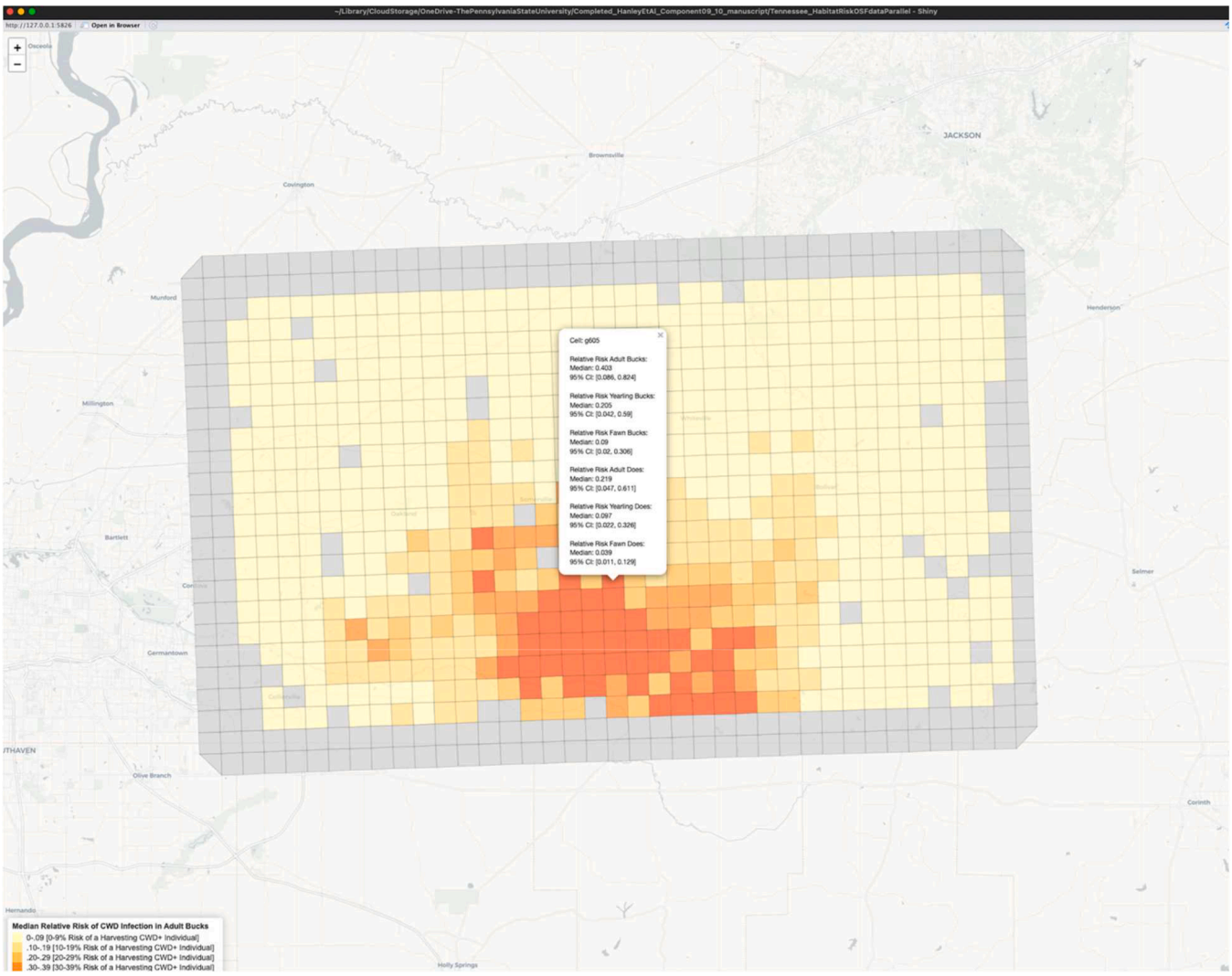


**Fig. 2.** The relative risk map in the *Habitat Risk* for adult males (Adult Bucks) for chronic wasting disease in white-tailed deer in southwest Tennessee, USA. Relative risk maps are available for the entire sampling grid through the tabs at top for adult male (Adult Buck), adult female (Adult Doe), yearling male (Yearling Buck) and female (Yearling Doe), and fawn male (Fawn Buck) and female (Fawn Doe) deer, or the risk by population segment is comparable in any cell by clicking on the cell to open its label.

CWD+ deer over the raster images of *elevation, slope, forest, streams, clay, open*, and *developed* in the study area. *Disease surveillance* data may be further partitioned by *sex* or *age*.

### 4.3. Relative risk for cwd by deer cohort

*Relative Risk Maps* tab reveals the median estimated risk, calculated as a proportion and percentage risk, and 95 % credible interval of harvesting a CWD+ deer for each grid cell in the study area (Fig. 2). Statistical estimations are displayed in an interactive map for adult males, adult females, yearling males, yearling females, fawn males, and fawn females, or a comparison may be shown among population segments for each cell by clicking the map to open the cell's label.

### 4.4. Model selection

*Model Selection* tab displays the 25 candidate model structures and their notation, listing the models in order of rank (relative fit to the data, in descending order by $_{\Delta}$DIC, where the best model has a $_{\Delta}$DIC = 0). The tab further displays for each model $\overline{D}$ which represents the posterior mean of the deviance (Evans et al., 2016); p$D$ which represents the effective number of parameters in the posterior distribution (equal to the variance of the deviance divided by 2 (Sturtz et al., 2005); DIC which represents the Deviance Information Criterion (Spiegelhalter et al., 2002); and $_{\Delta}$DIC, which represents the difference between the DIC value and the smallest DIC value among all models compared (Evans et al., 2016). Because the software is pre-programmed to run demographic and environmental covariates as presented in Table 1, running more or

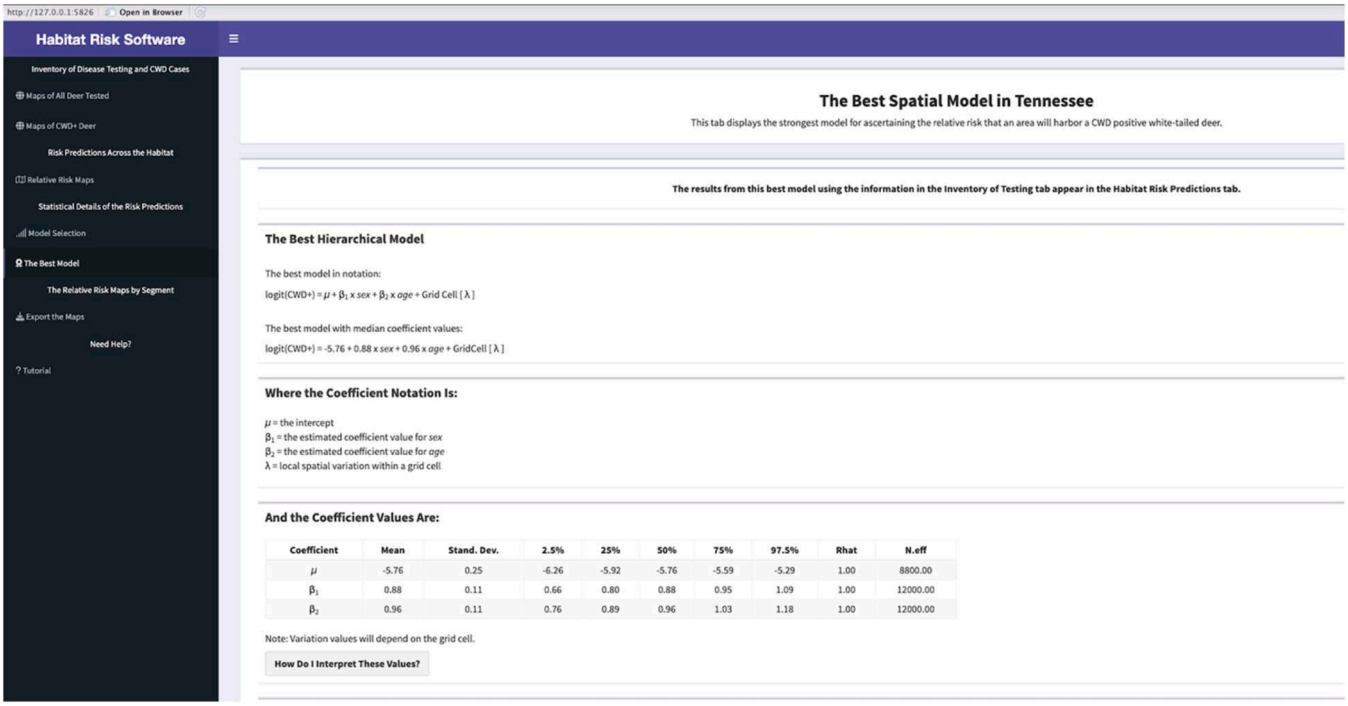


**Fig. 3.** Mean, median, standard deviation, and 95 % credible interval estimates for the best-fitting model (#20) using surveillance and environmental data from Tennessee, US. The parameter μ defines the baseline infection odds for an area harboring a CWD-positive female fawn white-tailed deer; $\beta_1$ represents the estimated coefficient for *sex* (male or female); $\beta_2$ represents the estimated coefficient for *age* (fawn, yearling, or adult); Rhat represents the diagnostic used to ensure that the Markov chain Monte Carlo chain has run a sufficient number of iterations (Brooks and Gelman 1998; Sturtz et al. 2005), when Rhat is equal to 1, the parameter has successfully converged to its appropriate posterior distribution; N.eff represents the effective sample size (Sturtz et al. 2005).

different models or adding additional covariates (e.g., proportion developed habitat) would require considerable changes to the software within each script.

### 4.5. Best model

*The Best Model* tab reveals the mathematical structure, and the coefficient value estimates (and their uncertainty) of the model most supported by data when DIC is compared (Fig. 3). The tab further displays convergence diagnostics, trace plots, and correlation plots generated when the MCMC process was completed for the best model.

### 4.6. Export maps

*Export Relative Risk Maps* tab allows the user to scroll, pan, and zoom the *Relative Risk Maps* for the population segment of interest in preparation for a download onto a local machine.

### 4.7. Tutorial tab

*Tutorial* tab displays brief information about the *Habitat Risk* software. We note that the location of this tutorial at the end of the software as well as location of other tabs on the *Habitat Risk* software were organized to satisfy agency requests.

### 4.8. Command center

An additional option for users would be to conduct the entire workflow combining scripts 1 to 3 using the script: *4_Tennessee_Command_Center*. Most users would find it more valuable to start with individual scripts to learn the process and prepare data for their needs. Advanced users may find it helpful to prepare data and run models using a single effort that this script provides.

## 5. Conclusions

The framework to examine disease presence in free-ranging wildlife populations, using Bayesian hierarchical modeling, ascertained how disease distribution may be related to environmental characteristics and assessed region-wide area and host-level variables while adjusting for additional covariates (Clayton and Kaldor, 1987; Besag et al., 1991; Waller et al., 1997; Banerjee et al., 2004; Farnsworth et al., 2006; Lawson et al. 2009). *Habitat Risk* provides a user-friendly workflow of the predictable steps of the Bayesian hierarchical modeling process and can be used with any timeframe of data, provided both types of input data (*disease surveillance* and *environmental*) exist for selected years. While *Habitat Risk* streamlines much of the predictable and repeated programmatic portions of such a complicated analysis, it also provides researchers easy access to these tools to garner localized information about the status of CWD within a defined area or to learn disease epidemiology using Bayesian hierarchical modeling.

Although there are potential hazards in automating an otherwise technical process, *Habitat Risk* requires the user to prepare data appropriately and review diagnostics during the process of executing the model in three crucial places: selection of the extent of the sampling grid, model selection process, and interpretation of the diagnostics. The

selection of the sampling grid must consider the signal-to-noise ratio, meaning that extraneous uncertainty can deleteriously influence modeling power and predictive performances. Thus, selection of the boundaries of the sampling grid relies on the geographic distribution of deer and would be most successful when positive or not detected results have few gaps with no locations and by deleting records with missing data in some records (e.g., sex, age, disease status) prior to subsampling observations for inclusion in modeling efforts. As well, because *Habitat Risk* was programmed *a priori* to select the model with the lowest relative DIC, the workflow cannot accommodate special analytical cases where model averaging is more appropriate than a static decision rule (Banner and Higgs, 2016; Hoeting et al., 1999). It must be externally verified that the model with the lowest DIC is indeed most appropriate given comparative performance of the remaining models in the candidate set. Finally, *Habitat Risk* displays to the user the diagnostic plots and summaries to ensure that parameter estimates ("the posteriors") of the best model were generated as intended (i.e., in a statistically appropriate way). The interface will not interpret these diagnostics on behalf of the user, however, nor is it programmed to halt display of the best model if computational assumptions have not been met. The interpretation of these diagnostics must be done carefully to ensure that all modeling assumptions have been met, and therefore that the displayed results are not misleading or invalid. Detailed directions are cited for each step in the Readme file of the software (Hanley et al., 2021). Furthermore, *Habitat Risk* can be rerun when new data becomes available, which may aid researchers in managing information flow given dynamic disease landscapes and public concern.

During completion of *Habitat Risk*, we discovered that it may be feasible to provide additional extant models into similar computational infrastructures to forge a future that more strongly links highly technical statistical or epidemiological analyses with localized wildlife disease data. Efforts to increase workflow efficiency may better translate technical scientific methods to broader users, which may aid researchers in enhancing the utility of models in wildlife management.

## CRediT authorship contribution statement

**W. David Walter:** Writing – review & editing, Writing – original draft, Visualization, Validation, Supervision, Software, Resources, Project administration, Methodology, Investigation, Funding acquisition, Formal analysis, Data curation, Conceptualization. **Brenda Hanley:** Writing – review & editing, Writing – original draft, Visualization, Validation, Software, Formal analysis, Data curation, Conceptualization. **Cara E. Them:** Writing – review & editing, Writing – original draft, Visualization, Validation, Software, Resources, Data curation. **Corey I. Mitchell:** Writing – review & editing, Writing – original draft, Visualization, Validation, Software, Resources. **James Kelly:** Writing – review & editing, Writing – original draft, Project administration, Funding acquisition, Data curation, Conceptualization. **Daniel Grove:** Writing – review & editing, Writing – original draft, Project administration, Investigation, Data curation, Conceptualization. **Nicholas Hollingshead:** Writing – review & editing, Writing – original draft, Visualization, Validation, Software, Resources, Formal analysis, Data curation. **Rachel C. Abbott:** Writing – review & editing, Writing – original draft, Software, Resources, Investigation, Formal analysis, Data curation, Conceptualization. **Krysten L. Schuler:** Writing – review & editing, Writing – original draft, Resources, Project administration, Methodology, Investigation, Funding acquisition, Formal analysis, Data curation, Conceptualization.

## Declaration of competing interest

The authors declare that they have no known competing financial interests or personal relationships that could have appeared to influence the work reported in this paper.

## Data availability

The R code is available as scripts on GitLab (https://doi.org/10.5066/P9541B7T) and state-specific code is available on eCommons (Hanley et al. 2021). Data for use in the R code is available on ScienceBase (https://www.sciencebase.gov/catalog/item/64de6780d34e5f6cd5535071).

## Acknowledgments

We thank T. Evans for his assistance on development of R code using *R2WinBUGS*, J. Fleegle, J. Peaslee, A. Korman, and two anonymous professionals for their helpful suggestions for improvement regarding functionality of the user interface. Any use of trade, firm, or product names is for descriptive purposes only and does not imply endorsement by the U.S. Government.

This Project was funded by a Multistate Conservation Grant # F23AP00488-00, a program funded from the Wildlife and Sport Fish Restoration Program, and jointly managed by the U. S. Fish and Wildlife Service and the Association of Fish and Wildlife Agencies.

## References


Association of Fish and Wildlife Agencies [AFWA], 2018. AFWA Best Management Practices for Prevention, Surveillance, and Management of Chronic Wasting Disease. https://www.fishwildlife.org/application/files/5215/3729/1805/AFWA_CWD_BMPS_12_September_2018_FINAL.pdf. Accessed: 16 February 2023.

Banerjee, S., Carlin, B.P., Gelfand, A.E., 2004. Hierarchical Modeling and Analysis For Spatial Data. Chapman and Hall/CRC, New York.

Banner, K.M., Higgs, M.D., 2016. Considerations for assessing model averaging of regression coefficients. Ecol. Appl. 27 (1), 78–93. https://doi.org/10.1002/eap.1419.

Besag, J., York, J., Mollie, A., 1991. Bayesian image restoration, with two applications in spatial statistics. Ann. Inst. Stat. Math. 43 (1), 1–59.

Brooks, S.P., Gelman, A., 1998. General methods for monitoring convergence of iterative simulations. J. Computational Graphical. Stats. 7, 434–455.

Burnham, K.P., Anderson, D.R., 2002. Model Selection and Multimodel inference: a Practical Information-Theoretic Approach. Springer-Verlag, New York, New York, USA.

Centers for Disease Control and Prevention [CDC]. 2021. Chronic wasting disease (CWD) occurrence and prion diseases. cdc.gov/prions/cwd/index.html Accessed: 16 February 2023.

Chang, W., J. Cheng, J. Allaire, C. Sievert, B. Schloerke, Y. Xie, J. Allen, J. McPherson, A. Dipert, B. Borges. 2016. Shiny: web application framework for R. https://CRAN.R-project.org/package=shiny. Accessed: 16 February 2023.

Clayton, D., Kaldor, J., 1987. Empirical bayes estimates of age-standardized relative risks for use in disease mapping. Biometrics 43 (3), 671–681.

Cornell Wildlife Health Laboratory [CWHL], 2021. Surveillence Optimization Project For Chronic Wasting Disese [SOP4CWD]. cwhl.vet.cornell.edu/project/sop4cwd. Accessed: 16 February 2023.

Dewitz, J. 2019. National land cover database (NLCD) 2016 products: U.S. Geological Survey data release. 10.5066/P96HHBIE Accessed: 16 February 2023.

Eberly, L.E., Carlin, B.P., 2000. Identifiability and convergence issues for Markov chain Monte Carlo fitting of spatial models. Stat. Med. 19, 2279–2294.

Evans, T.S., Kirchgessnerr, M.S., Eyler, B., Ryan, C.W., Walter, W.D., 2016. Habitat influences distribution of chronic wasting disease in white-tailed deer. J. Wildl. Manage. 80 (2), 284–291.

Farnsworth, M.L., Hoeting, J.A., Hobbs, N.T., Miller, M.W., 2006. Linking chronic wasting disease to mule deer movement scales: a hierarchical bayesian approach. Ecol. Appl. 16 (3), 1026–1036.

Ferreira, M., Filipe, A.F., Bardos, D.C., Magalhaes, M.F., Beha, P., 2016. Modeling stream fish distributions using interval-censored detection times. Ecol. and Evol. 6 (15), 5530–5541.

Gelman, A., Carlin, J.B., Stern, H.S., Rubin, D.B., 2004. Bayesian Data Analysis. Chapman and Hall/CRC, New York.

Geweke, J. 1992. Evaluating the Accuracy of Sampling-Based Approaches to Calculating Posterior Moments. In Bayesian Statistics 4 (ed JM Bernardo, JO Berger, AP Dawid, and AFM Smith). Clarendon Press, Oxford, UK.

Gesch, D., 2007. The National Elevation Dataset. In: Maune, D. (Ed.), Digital Elevation Model Technologies and Applications: The DEM Users Manual No. Second. American Society for Photogrammetry and Remote Sensing, Bethesda, pp. 99–118.

Gilbert, F.F., 1966. Aging white-tailed deer by annuli in the cementum of the first incisor. J. Wildl. Manage. 30, 200–202.

Grear, D.A., Samuel, M.D., Langenberg, J.A., Keane, D., 2006. Demographic patterns and harvest vulnerability of chronic wasting disease infected white-tailed deer in Wisconsin. J. Wildl. Manage. 70 (2), 546–553.

Hanley, B., C.I. Mitchell, W.D. Walter, J. Kelly, R.C. Abbott, N. Hollingshead, L. Miller, K. Schuler. 2021. Habitat Risk Software 10.7298/rcz8-nw50. Accessed: 16 February 2023.

Hefley, T.J., Hooten, M.B., Russell, R.E., Walsh, D.P., Powell, J.A., 2017. When mechanism matters: bayesian forecasting using models of ecological diffusion. Ecol. Lett. 20 (5), 640–650. https://doi.org/10.1111/ele.12763.

Heidelberger, P., Welch, P.D., 1983. Simulation run length control in the presence of an initial transient. Operations Res 31, 1109–1144.

Hethcote, H.W., 1989. Three basic epidemiological models. In: Levin, S.A., Hallam, T.G., Gross, L.J. (Eds.), Applied Mathematical Ecology. Springer Berlin Heidelberg, Berlin, Heidelberg, pp. 119–144.

Hoeting, J.A., Madigan, D., Raftery, A.E., Volinsky, C.T., 1999. Bayesian model averaging: a tutorial. Stat. Sci. 14 (4), 382–417.

Horn, B.K.P., 1981. Hill shading and the reflectance map. Proc. IEEE 69 (1), 14–47. https://doi.org/10.1109/PROC.1981.11918.

Keane, D.P., Barr, D.J., Bochsler, P.N., Hall, S.M., Gidlewski, T., O'Rourke, K.I., Spraker, T.R., Samuel, M.D., 2008. Comparison of retropharyngeal lymph node and obex region of the brainstem in detection of chronic wasting disease in white-tailed deer (*Odocoileus virginianus*). J. Vet. Diagn. Invest. 20, 58–60.

Kelly, A.C., Mateus-Pinilla, N.E., Brown, W., Ruiz, M.O., Douglas, M.R., Douglas, M.E., Shelton, P., Beissel, T., Novakofski, J., 2014. Genetic assessment of environmental features that influence deer dispersal: implications for prion-infected populations. Popul. Ecol. 56 (2), 327–340.

Lawson, A.B., 2009. Bayesian Disease mapping: Hierarchical Modeling in Spatial Epidemiology. Chapman and Hall/CRC, Boca Raton.

Lunn, D.J., Thomas, A., Best, N., Spiegelhalter, D., 2000. WinBUGS - A bayesian modelling framework: concepts, structure, and extensibility. Stat. Comp. 10, 325–337.

McKay, L., Bondelid, T., Devald, T., Johnston, J., Moore, R., Rea, A., 2012. NHDPlus Version 2: User Guide. https://www.epa.gov/system/files/documents/2023-04/NHDPlusV2_User_Guide.pdf. Accessed: 16 February 2023.

Miller, M.W., Conner, M.M., 2005. Epidemiology of chronic wasting disease in free-ranging mule deer: spatial, temporal, and demographic influences on observed prevalence patterns. J. Wildl. Dis. 41 (2), 275–290.

Miller, W.L., Miller-Butterworth, C.M., Diefenbach, D.R., Walter, W.D., 2020. Assessment of spatial genetic structure to identify populations at risk for infection of an emerging epizootic disease. Ecol. Evol. 10 (9), 3977–3990. https://doi.org/10.1002/ece3.6161.

Mitchell, C.I., W.D. Walter, N. Hollingshead, K. Schuler. 2021. Processing of geospatial data for the Habitat Risk software. https://ecommons.cornell.edu/handle/1813/104257. Accessed: 16 February 2023.

Mollison, D., 1977. Spatial contact models for ecological and epidemic spread. J. Roy. Stat. Soc. Ser. B. (Method.) 39 (3), 283–313. https://doi.org/10.1111/j.2517-6161.1977.tb01627.x.

Osnas, E.E., Heisey, D.M., Rolley, R.E., Samuel, M.D., 2009. Spatial and temporal patterns of chronic wasting disease: fine-scale mapping of a wildlife epidemic in Wisconsin. Ecol. Appl. 19 (5), 1311–1322.

Plummer, M., Best, N., Cowles, K., Vines, K., 2006. CODA: convergence diagnosis and output analysis for. MCMC. R News 6, 7–11. cran.r-project.org/doc/Rnews/Rnews_2006-1.pdf#page=7.

Raftery, A.E., Lewis, S.M., 1992. One long run with diagnostics: implementation strategies for Markov chain Monte Carlo. Statistical Sci 7, 493–497.

Roy, V., 2020. Convergence diagnostics for Markov chain Monte Carlo. Ann. Rev. Stat. Apps. 7, 387–412.

Schuler, K.L., Hollingshead, N., Kelly, J.D., Applegate, R.D., Yoest, C., 2018. A Risk-Based Weighted Surveillance Plan. Tennessee Wildlife Resources Agency.

Severinghaus, C.A., 1949. Tooth development and wear as criteria of age in white-tailed deer. J. Wildl. Manage. 13 (2), 195–216.

Spiegelhalter, D.J., Best, N.G., Carlin, B.P., van der Linde, A., 2002. Bayesian measures of model complexity and fit. J. Roy. Stat. Soc. Ser. B. (Stat. Method.) 64 (4), 583–639.

Soil Survey Staff. 2020. Gridded National Soil Survey Geographic (gNATSGO) Database for the Conterminous United States. nrcs.app.box.com/v/soils Accessed: 16 February 2023.

Stem, J.E. . 1990. State Plane Coordinate System of 1983. https://www.ngs.noaa.gov/library/pdfs/NOAA_Manual_NOS_NGS_0005.pdf Accessed: 16 February 2023.

Storm, D.J., Samuel, M.D., Rolley, R.E., Shelton, P., Keuler, N.S., Richards, B.J., Van Deelen, T.R., 2013. Deer density and disease prevalence influence transmission of chronic wasting disease in white-tailed deer. Ecosphere 4 (1), 10. https://doi.org/10.1890/ES12-00141.1.

Sturtz, S., Ligges, U., Gelman, A., 2005. R2WinBUGS: a package for running WinBUGS from R. J. Stat. Softw. 12 (3), 1–16.

R Core Team. 2020. R: a language and environment for statistical computing. https://www.R-project.org/Accessed: 16 February 2023.

Tennessee Wildlife Resources Agency [TWRA], 2023. CWD in Tennessee. https://www.tn.gov/content/tn/twra/hunting/cwd/cwd-in-tennessee.html. Accessed: 16 February 2023.

United States Geological Survey [USGS]. 2023. Expanding distribution of chronic wasting disease. usgs.gov/centers/nwhc/science/expanding-distribution-chronic-wasting-disease?qt-science_center_objects=0#qt-science_center_objects Accessed: 16 February 2023.

Waller, L.A., Carlin, B.P., Xia, H., Gelfand, A.E., 1997. Hierarchical spatio-temporal mapping of disease rates. J. Am. Stat. Assoc. 92 (438), 607–617.

Walter, W.D., Evans, T.S., Stainbrook, D., Wallingford, B.D., Rosenberry, C.S., Diefenbach, D.R., 2018. Heterogeneity of a landscape influences size of home range in a. North American cervid. Sci. Rep. 8 (1), 14667. https://doi.org/10.1038/s41598-018-32937-7.

Walter, W.D., Smith, R., Vanderklok, M., VerCauteren, K.C., 2014. Linking bovine tuberculosis on cattle farms to white-tailed deer and environmental variables using Bayesian hierarchical analysis. PLoS One 9 (3), e90925.

Walter, W.D., Walsh, D.P., Farnsworth, M.L., Winkelman, D.L., Miller, M.W., 2011. Soil clay content underlies prion infection odds. Nat. Commun. 2 (200), 1–6.

Wieczorek, M. 2014. Area- and depth- weighted averages of Selected SSURGO Variables For the Conterminous United States and District of Columbia. 866, Reston, VA.

Williams, E.S., Miller, M.W., Kreeger, T.J., Kahn, R.H., Thorne, E.T., 2002. Chronic wasting disease of deer and elk: a review with recommendations for management. J. Wildl. Manage. 66 (3), 551–563.

Williams, E.S., Young, S., 1980. Chronic wasting disease of captive mule deer: a spongiform encephalopathy. J. Wildl. Dis. 16 (1), 89–96.

Zar, J.H., 1996. Biostatistical Analysis. Prentice Hall, Upper Saddle River, New Jersey, USA.